Antennas for the array-based deep space network: Current status and future designs

Conference Paper *in* IEEE Aerospace Conference Proceedings · April 2005

DOI: 10.1109/AERO.2005.1559405 · Source: IEEE Xplore

CITATION
1

READS
220

2 authors:

W.A. Imbriale
California Institute of Technology
154 PUBLICATIONS **1,449** CITATIONS
SEE PROFILE

Eric Gama
California Institute of Technology
8 PUBLICATIONS **22** CITATIONS
SEE PROFILE

Antennas for the Array-Based Deep Space Network: Current Status and Future Designs

William A. Imbriale and Eric Gama
Jet Propulsion Laboratory, California Institute of Technology
4800 Oak Grove Drive
Pasadena, CA 91109
818-354-5172
William.A.Imbriale@jpl.nasa.gov

Abstract—Development of very large arrays[1,2] of small antennas has been proposed as a way to increase the downlink capability of the NASA Deep Space Network (DSN) by two or three orders of magnitude thereby enabling greatly increased science data from currently configured missions or enabling new mission concepts. The current concept is for an array of 400 x 12-m antennas at each of three longitudes. The DSN array will utilize radio astronomy sources for phase calibration and will have wide bandwidth correlation processing for this purpose. NASA has undertaken a technology program to prove the performance and cost of a very large DSN array. Central to that program is a 3-element interferometer to be completed in 2005. This paper describes current status of the low cost 6-meter breadboard antenna to be used as part of the interferometer and the RF design of the 12-meter antenna.

TABLE OF CONTENTS

1. INTRODUCTION

The baseline breadboard antenna is a 6-*meter hydroformed symmetrically shaped dual reflector system utilizing Gregorian optics*. Hydroforming is the process of forming aluminum to a rigid and precise mold by using a fluid or gas under pressure. Three of these reflectors with rms less than 0.2 mm have been delivered to JPL. They have been integrated with a backup structure that utilizes 9 equally spaced aluminum struts connecting a center yoke to the rim of the dish. The pedestal consists of a central pipe tucked under the dish with a central bearing for azimuth motion and a jackscrew for elevation control. The first antenna has been assembled and is currently undergoing testing. The results of the initial reflector surface measurements are presented.

The 6-meter design is described in reference [1, 2] and consisted of Gregorian optics modified from an original maximum gain design to a maximum gain divided by noise temperature (G/T) design. For maximum flexibility in the testing and evaluation phase of the project, Gregorian optics was selected to allow tests with prime focus feeds without removing the subreflector. However, for the antenna that will actually be used in the final array, G/T is the overriding requirement. The question then becomes, which design, Gregorian or Cassegrain, provides the maximum G/T? A tradeoff study was performed which concluded that, at least for the case of designs using very low noise amplifiers, Cassegrain optics is superior to Gregorian optics for a maximum G/T design. One additional constraint of the 12-meter design was that it was to use the same feed design [3] as the 6-meter antenna. The tradeoff study and final selected design is described.

2. THE 6-METER BREADBOARD ANTENNA

The design of the 6-meter Breadboard Antenna is well documented in references [1–4] and will only be briefly summarized here.

The RF-design utilizes Gregorian optics in which the main reflector shape comes from an original maximum gain design but the subreflector was modified so that the final design is a maximum G/T design [1].

The feed is a dual frequency horn (Figure 1) covering the X (8–9 GHz) and Ka (30–40 GHz) bands. The X-band is a coaxial waveguide fed corrugated horn and Ka-band utilizes a dielectric rod in the center of the corrugated horn [3].

The cryogenics system (Figure 2) cools the dual frequency feed system equipped with HEMT low noise amplifiers and the associated support electronics. The cryocooler is a CTI Cryogenics model 350 that produces 3 watts of cooling at 15K. The vacuum housing is constructed using aluminum tubing. It eliminates welding and the problems associated

[1] 0-7803-8870-4/05/$20.00© 2005 IEEE
[2] IEEEAC paper #1188, Version 4, Updated January 20, 2005

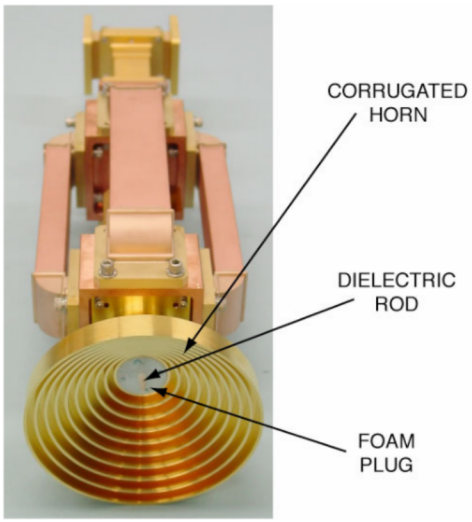

Figure 1. The Dual Frequency Feed

Figure 2. The Cryogenics Package

with vacuum leaks and warping. The end plate for the vacuum housing uses the standard machined aluminum plate design. The plate is fitted with simple gland-seal O-ring connections. The feed is supported mechanically from the base with G-10 fiberglass supports. The radiation shield is a simple rolled cone. A foam backed Kapton membrane was chosen for the vacuum window [4].

The critical technology in the mechanical system for the reflector is the dish manufactured from a process called Hydroforming. This is the process of forming aluminum to a rigid and precise mold by using a fluid or gas under pressure. For the DSN breadboard, the dish aperture is 6.048 m or 20 ft. The dish is connected to a rigid Truss Structure at two places. The dish is hard mounted to the Truss Structure at its center. Spars connect the rim of the Dish to the rear of the Truss Structure. The Truss Structure is connected to the Petal Yoke at the elevation pivot point. There is a linear actuator or Jackscrew mechanism attached to the rear of the Yoke. As the Jackscrew extends or contracts the elevation of the Main Dish is changed. The Yoke is connected to the Petal Base through a Slew Bearing, with gears on the outer ring. Two opposing motors, mounted inside the Yoke, drive the Azimuth Axis. The Dish, Truss Structure and Spars are made of aluminum. The Yoke and Pedestal Base are made of steel. The total weight of the antenna is approximately 8500 lbs. See Figure 3 for a drawing of the complete antenna and reference [2] for more details on the mechanical design.

3. Gravity and Thermal Distortion

Surface accuracy of the dish after manufacturing must be less than 0.2 mm rms. For either gravity, wind or temperature the change in rms cannot be greater than 0.13 mm.

The dish was assembled inside a high-bay building and initial measurements were made of the as manufactured shape as well as the gravity performance as a function of elevation angle. Figure 4 is a picture of the front surface of the dish with the targets used for the photogrammetry measurements of the dish surface. This is prior to installing the feed, subreflector and subreflector support. Figure 5 is a graph of the best-fit surface with the dish pointed vertically (90 degrees elevation). The surface RMS is aa mm. The dish was measured approximately every 22 degrees down to an elevation of 20 degrees (the lowest elevation angle that could be accommodated inside the building). There were two sets of measurements and the data is summarized in Table 1. Figure 6 is a graph of the difference between 90 and 20 degrees elevation. The RMS is less than 0.05 mm (2 mils). As seen from the table and graph, the dish exhibits excellent performance as a function of elevation angle.

The subreflector and subreflector supports were installed and the dish re-measured at 45 degrees and the RMS was 0.3239 mm (12.75 mils), virtually the same as the no subreflector case.

The antenna was partially disassembled, transported to the Mesa and reassembled (Figure 7). An initial measurement was made at nighttime (elevation 45 degrees) since it was an isothermal condition similar to Building 18. The graph of the best-fit surface is shown in Figure 8. The RMS is now 0.4531 mm (17.84 mils), indicating that there was some degradation caused during transport and reassembly. This problem is currently being investigated. However, the dish was also measured at 10 degrees elevation and the

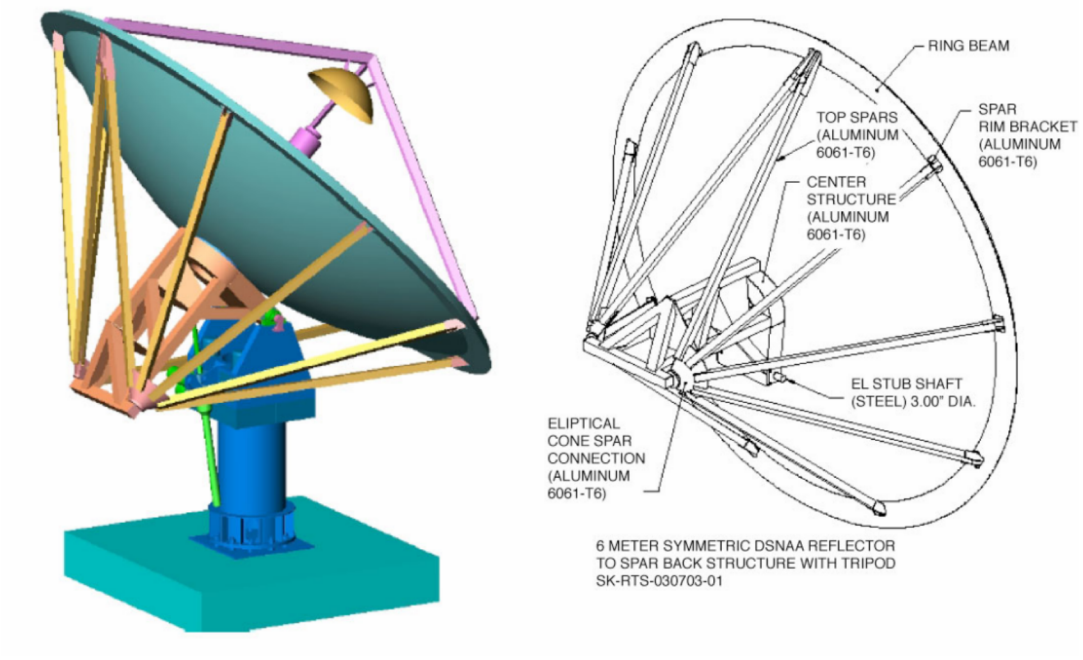

Figure 3. The 6-meter Breadboard Antenna

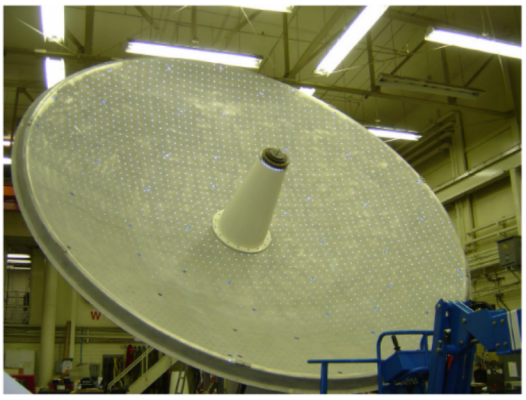

Figure 4. Front Surface with Photogrammetry Targets

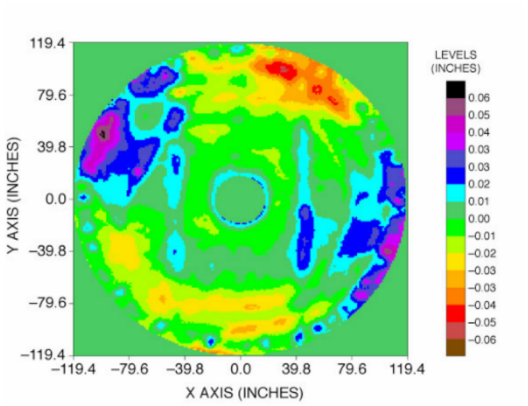

Figure 5. Best-fit Surface at 90 Degrees Elevation

Table 1. RMS performance as a function of elevation angle

Elevation Angle (degrees)	Measurement 1		Measurement 2	
	RMS (mils)	RMS (mm)	RMS (mils)	RMS (mm)
20.0	12.67	0.3218	12.56	0.3213
32.5	12.45	0.3162	12.64	0.3211
45.0	12.91	0.3279	12.44	0.3160
67.5	12.68	0.3221	12.66	0.3216
90.0	12.19	0.3096	12.82	0.3256

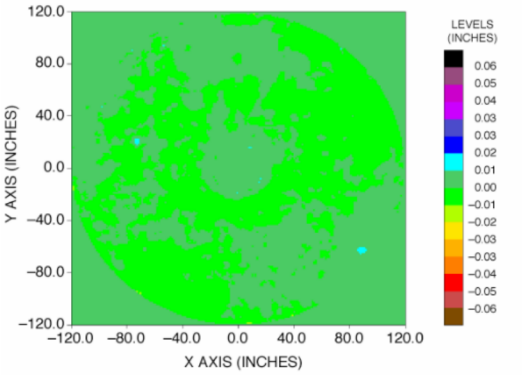

Figure 6. Difference Between 90 and 20 Degrees Elevation

Figure 7. Antenna on the Mesa

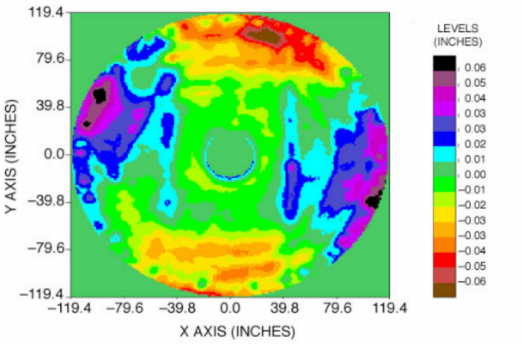

Figure 8. Nighttime Measurement on the Mesa

difference from 45 degrees elevation was only 0.036 mm (1.4 mils) continuing the excellent performance for gravity effects.

A measurement was made with the dish in full sun and the best-fit surface shown in Figure 9. The RMS is now 0.574 mm (22.60 mils) indicating a significant thermal effect. This thermal variation was expected since the dish is not painted with the traditional white paint. There was a desire to measure dishes with and without paint to determine if the cost of painting the surface could be eliminated. The difference between the full sun and nighttime case is shown in Figure 10. The RMS of the difference between the two cases is 0.3352 mm (13.2 mils), which exceeds the thermal requirement, indicating that it will be necessary to paint the dishes.

4. Optimizing for Maximum G/T

For the 12-meter antenna the requirement is to maximize the G/T ratio. This then minimizes the number of antennas required to achieve a specified G/T for the array. This section describes the technique used to optimize the design for G/T.

In a dual reflector antenna geometrical optics shaped for maximum gain, the main reflector is illuminated by the subreflector in such a way as to produce a uniform aperture distribution [5]. This utilizes a subreflector pattern that has a high edge taper that is truncated to zero at the edge of the main reflector. Unfortunately, due to diffraction effects, a real subreflector pattern does not go to zero at the main reflector edge and there is substantial spillover in the rear direction. This spillover sees the hot earth and consequently increases the noise temperature of the antenna system. The DSN has typically dealt with this problem in two ways. 1) Select the uniform illumination function of the main reflector to be less than the physical aperture, thus using the remainder of the aperture as a noise shield and reducing the spillover energy that falls on the hot earth or 2) Select the illumination function to be uniform to a give radius and then

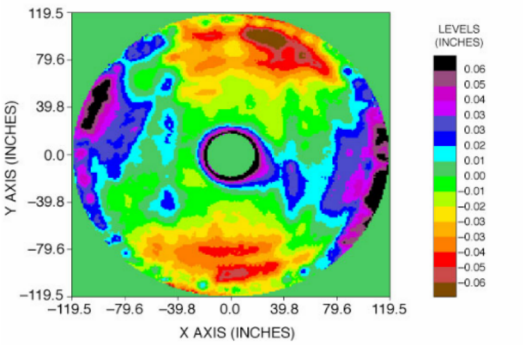

Figure 9. Full Sun Measurement on the Mesa

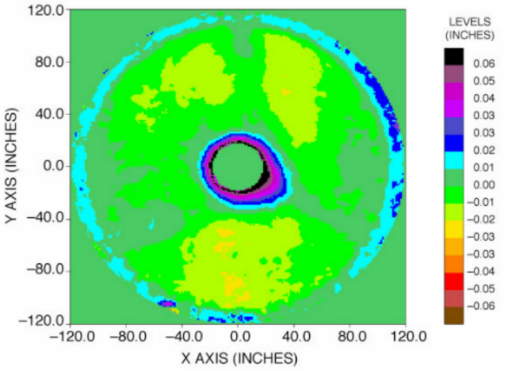

Figure 10. Difference Between Full Sun and Nighttime

taper it to zero at the reflector edge, also reducing the rear spillover. The 70-meter antennas, the HEF, DSS-13 and the ARST antennas used method 1) and the operational BWG antennas used method 2). Both methods yield virtually identical results for G/T. This study will use method 1.

5. Cassegrainian or Gregorian

The study will be done in two parts. First part will determine whether there is any G/T performance difference between the two types of designs, and if so, the second part will refine the design of the selected choice to best match the mechanical design.

The coordinate system used for shaping is shown in Figure 11. Parameters available for the design are the subreflector radius k, the main reflector radius x_m, the subreflector edge angle θ_m, the central hole diameter, the feed radiation pattern, and the location of the horn focus "a". Since an existing feed is to be used, the feed radiation pattern is given and will be approximated by a cos(θ)**Q pattern with Q = 4.96. The choice of "a" can be determined by minimizing the difference between the resulting shape and a given focal length to diameter ratio (F/D). Since it is known that the G/T performance is only minimally effected by the focal length, a F/D = 0.375 was selected to be similar to the breadboard antenna. For the initial study, a 10% subreflector diameter of 1.2 meters was selected with a corresponding central hole diameter also 1.2 meters. The two parameters to be optimized were then the diameter for uniform illumination and the subreflector edge angle. Tables 2 and 3 compare the performance of a Cassegrainian and Gregorian design. For the G/T computation an amplifier noise temperature of 15K was assumed and the gain calculation did not include all the estimated losses that would be common to both designs. Since the spillover is greatest at the lowest frequency, the design was optimized at the lowest DSN X-band frequency of 8.4 GHz.

As can be clearly seen from the two tables, there is a clear advantage for the Cassegrain design. The optimum G/T for the Gregorian design is 47.29 dB, while the optimum G/T for the Cassegrain design is 0.82 dB greater at 48.11 dB. Additional calculations were made for a larger subreflector (1.8 meters) and for different F/D ratios but the substantial advantage of the Cassegrain design of about 0.7–0.8 dB remained. Method 2 (as described above) was also examined, but, as expected, the difference in performance between the two methods for optimum G/T design was less than 0.1 dB. Hence, a Cassegrain design was chosen for the 12-meter reflector.

It is interesting to note that the peak gain of both designs is virtually identical. To understand why the Cassegrain design has the better G/T performance it is only necessary to look at the subreflector scatter patterns. Figure 12 shows the subreflector scatter patterns for the case of peak gain. Notice the substantial spillover for the Gregorian design. To reduce the spillover it is necessary to illuminate less of the main reflector, thus using the outer edge of the reflector as a noise shield. Figure 13 compares the scatter patterns for the case of optimum G/T. Notice the lower peak illumination and wider skirts to the pattern for the Gregorian case. It's also to be noted that this difference in G/T would be substantially smaller for a high noise amplifier.

6. Cassegrainian Design

To select the specific design parameters, G/T calculations were also made at Ka-band (32 GHz) and the results shown in Table 4.

In computing Table 4, the calculated feed patterns were used and an amplifier noise temperature of 15K for X-band and 35K for Ka-band was assumed. Either the 50 degree subreflector edge angle with a uniform illumination radius of 5.8 meters or the 55 degree subreflector edge angle with a uniform illumination radius of 5.8 meters appears to offer a good comprise between X- and Ka-band performance. However, the smaller angle is preferred because the feed is

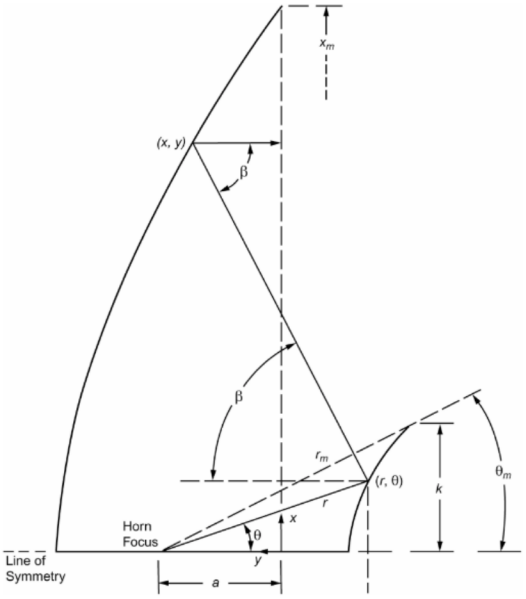

Figure 11. Coordinate System for Shaping

Table 2. Gregorian Design

Radius, m	Gain, dB	T_a, K	G/T
45 Degree Subreflector Edge Angle			
6.0	59.85	14.93	45.09
5.8	59.87	7.78	46.29
5.6	59.72	3.91	46.95
5.4	59.44	2.02	47.13
5.2	59.08	1.20	46.99
50 Degree Subreflector Edge Angle			
6.0	59.97	17.86	44.81
5.8	60.01	8.78	46.25
5.6	59.82	3.86	47.07
5.4	59.49	1.70	47.26
5.2	59.11	0.89	47.10
55 Degree Subreflector Edge Angle			
6.0	60.03	21.07	44.46
5.8	60.08	10.18	46.07
5.6	59.84	4.03	47.05
5.4	59.46	1.49	47.29
5.2	59.07	0.65	47.17
60 Degree Subreflector Edge Angle			
6.0	60.04	24.02	44.13
5.8	60.11	11.76	45.83
5.6	59.81	4.32	46.94
5.4	59.39	1.34	47.25
5.2	58.99	0.53	47.09

Table 3. Cassegrain Design

Radius, m	Gain, dB	T_a, K	G/T
45 Degree Subreflector Edge Angle			
6.0	59.85	3.58	47.16
5.8	59.92	1.49	47.66
5.6	59.67	0.74	47.70
5.4	59.40	0.52	47.49
50 Degree Subreflector Edge Angle			
6.0	59.97	2.93	47.43
5.8	59.95	0.99	47.94
5.6	59.78	0.38	47.91
5.4	59.50	0.29	47.65
55 Degree Subreflector Edge Angle			
6.0	60.03	2.78	47.52
5.8	60.02	0.62	48.08
5.6	59.83	0.22	48.00
5.4	59.52	0.19	47.70
60 Degree Subreflector Edge Angle			
6.0	60.05	2.93	47.51
5.8	60.04	0.60	48.11
5.6	59.83	0.19	48.01
5.4	59.50	0.17	47.69

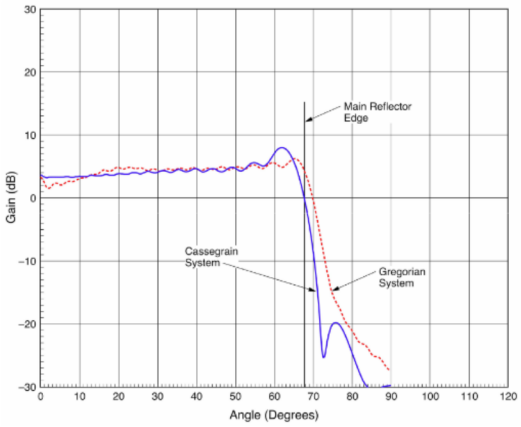

Figure 12. Subreflector Scatter Patterns—Peak Gain Case

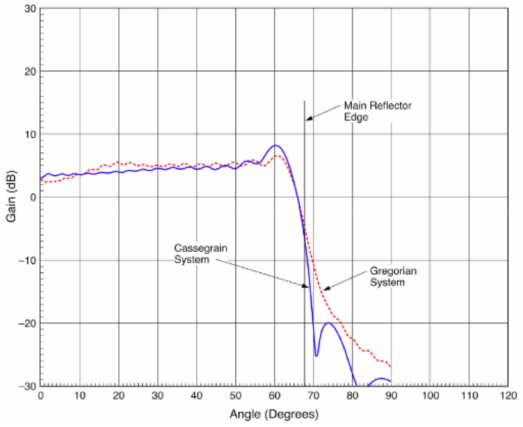

Figure 13. Subreflector Scatter Patterns at Peak G/T

further away from the subreflector posing less of a feed blockage problem.

To examine the F/D dependence, calculations were made for F/D = 0.35, 0.375 and 0.4 and the results summarized in Table 5. As can be seen from the table, there is virtually no difference in RF performance of the shaped system for different F/D ratios. The F/D ratio could then be selected based upon mechanical considerations. For similarity with the 6-meter design, an F/D = 0.375 was chosen. The vendor fabricating the 12-meter breadboard antenna was given the opportunity to change the F/D but declined.

When the geometry of the 50-degree subreflector edge angle and the 18.1-cm feed diameter is examined, it is seen (Figure 14a) that the ray from the center of the subreflector to the main reflector is blocked by the feed. It is necessary to use a 15% (1.8 m) diameter subreflector to provide sufficient feed spacing from the subreflector to prevent the feed blockage (Figure 14b). The final design is then a subreflector edge angle of 50 degrees, a uniform illumination radius of 5.8 meters and a 1.8-meter subreflector. The geometry is documented in JPL Control Drawing #9623454. Interestingly enough, for this design, the G/T at X-band is 48.13 dB, which is 0.01 dB higher than the largest value in Table 3.

7. G/T Estimates

The above calculations were done primarily for tradeoff comparisons and did not include all the estimated losses that would be common to all designs. The above results included the calculated losses from the PO programs and an estimated 15K noise temperature contribution from the low noise amplifier system at X-band and 35K at Ka-band. The purpose of this section is to provide a more complete G/T performance estimate including the expected uncertainties. The Performance estimates for the X- and Ka-band amplifiers can be found in Reference [1]. They are the wideband MMIC design. A typical estimate for the system noise temperature is shown in Table 6 and a typical gain budget is shown in Table 7. Estimated G/T is from 45.8 to 48.1 dB/K at X-band (8.4 GHz) and 53.4 to 55.3 dB/K at Ka-band (32 GHz).

8. Conclusions

The current status of the first 6-meter breadboard antenna has been described. It is currently operational and preliminary measurements of the surface contour as a function of elevation angle have been made.

In addition, for the 12-meter antenna design, it was demonstrated that a Cassegrain configuration would be approximately 0.7 dB better in G/T than a comparable Gregorian configuration.

Acknowledgment

The research was carried out at the Jet Propulsion Laboratory, California Institute of Technology, under a contract with the National Aeronautics and Space Administration.

References

[1] W. A. Imbriale and R. Abraham, "Radio Frequency Optics Design of the Deep Space Network Large Array 6-Meter Breadboard Antenna," *The Interplanetary Network Progress Report*, vol. 42-157, Jet Propulsion Laboratory, Pasadena, California, pp. 1–8, May 15, 2004. http://ipnpr/progress report/42-157/157E.pdf

[2] W. A. Imbriale, S. Weinreb, A. Feria, C. Porter, D. Hoppe, and M. Britcliffe, "The 6-Meter Breadboard Antenna for the Deep Space Network Large Array," *The Interplanetary Network Progress Report*, vol. 42-157, Jet Propulsion Laboratory, Pasadena, California, pp. 1–12, May 15, 2004. http://ipnpr/progress report/42-157/157M.pdf

[3] D. J. Hoppe and H. Reilly, "Simultaneous 8- to 9-GHz and 30- to 40-GHz Feed for the Deep Space Network Large Array," *The Interplanetary Network Progress Report*, vol. 42-157, Jet Propulsion Laboratory, Pasadena, California, pp. 1–16, May 15, 2004. http://ipnpr/progress report/42-157/157B.pdf

Table 4. G/T at X- and Ka-band for the Cassegrainian Design

Radius, m	X-band (8.4 GHz)			Ka-band (32 GHz)		
	Gain, dB	T_a, K	G/T	Gain, dB	T_a, K	G/T
45 Degree Subreflector Angle						
5.9	59.86	2.28	47.48	71.62	0.65	56.10
5.8	59.82	1.49	47.66	71.52	0.24	56.05
5.7	59.76	1.00	47.72	71.38	0.00	55.94
50 Degree Subreflector Angle						
5.9	59.98	1.63	47.77	71.70	0.09	56.24
5.8	59.95	0.99	47.94	71.57	0.00	56.14
5.7	59.88	0.55	47.97	71.43	0.00	55.99
55 Degree Subreflector Edge Angle						
5.9	60.04	1.37	47.90	71.73	0.19	56.27
5.8	60.02	0.62	48.08	71.59	0.00	56.15
5.7	59.94	0.31	48.09	71.44	0.00	56.00
60 Degree Subreflector Edge Angle						
5.9	60.07	1.37	47.93	71.74	0.05	56.29
5.8	60.04	0.60	48.11	71.58	0.21	56.11
5.7	59.96	0.29	48.12	71.44	0.17	55.97

Table 5. F/D Dependence for 5.8m Radius, 10% Sub and 50-Degree Angle

F/D	Gain, dB	T_a, K	G/T
0.35	59.95	0.98	47.92
0.375	59.95	0.99	47.94
0.40	59.95	1.01	47.91

[4] M. J. Britcliffe, T. R. Hanson, and M. M. Franco, "Cryogenic Design of the Deep Space Network Large Array Low-Noise Amplifier System," *The Interplanetary Network Progress Report*, vol. 42-157, Jet Propulsion Laboratory, Pasadena, California, pp. 1–13, May 15, 2004. http://ipnpr/progress report/42-157/157C.pdf

[5] W. A. Imbriale, *Large Antennas of the Deep Space Network,* John Wiley and Sons Inc., Hoboken, New Jersey, pp. 20–23, 2003.

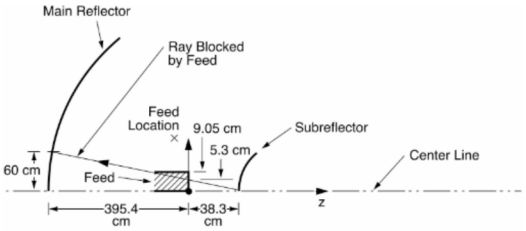

Figure 4a
10% Subreflector

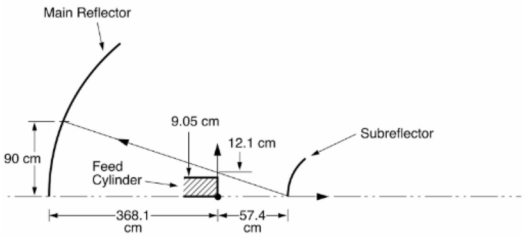

Figure 4b
15% Subreflector

Figure 14. Feed Blockage

Table 6. Typical Noise Temperature Budget

Element	Noise, K		Note
	X-band, 8.4 GHz	K-band, 32 GHz	
Cosmic background	2.5	2.0	Effective blackbody
Atmosphere	2.2	7.0	Goldstone (ave clear)
Forward spill	0.2	0.1	4% X-band, 1.5% Ka-band
Main reflector rear spill	0.3	1.0	
Main reflector I^2R	0.1	0.2	Aluminum
Subreflector I^2R	0.1	0.2	Aluminum
Quadripod scatter	2/4	2/4	Estimated
Feed/amplifier cont	6.1/12.4	18.6/30.2	See Reference [1]
Total Noise, K	13.5/21.8	31.1/44.7	

Table 7. Typical Efficiency Budget

Element	Efficiency		Note
	X-band, 8.4 GHz	K-band, 32 GHz	
P.O. computed	0.891	0.865	100% = 60.48 -X 100% = 72.09 -Ka
Main Reflector			
I^2R	0.999	0.999	
RMS	0.988	0.846	12 mils RMS
Subreflector			
I^2R	0.999	0.999	
RMS	0.999	0.982	4 mils RMS
Feed support blockage	0.85/0.9	0.85/0.9	Estimated
Feed VSWR	0.999	0.999	
Efficiency Gain (dB)	0.745/0.789 59.20/59.45	0.609/0.645 69.94/70.19	

BIOGRAPHY

William A. Imbriale *is a senior research scientist in the Communications Ground System Section at the Jet Propulsion Laboratory (JPL) in Pasadena, California. Since starting at JPL in 1980, he has led many advanced technology developments for large ground-station antennas, lightweight spacecraft antennas, and millimeter-wave spacecraft instruments. He has recently returned from a 6 month sabbatical at CSIRO in Australia where he worked with the Australian Telescope National Facility. He is currently working on the Deep Space Network Large Array, a concept to significantly increase the capability of the Deep Space Network (DSN) by arraying a large number of inexpensive small antennas. Earlier positions at JPL have included being the Assistant Manager for Microwaves in the Ground Antennas and Facilities Engineering Section and the Manager of the Radio Frequency and Microwave Subsystem Section.*

Prior to joining JPL in 1980, Dr. Imbriale was employed at the TRW Defense and Space Systems Group where he was the Subproject Manager for the Antennas of the TDRSS program.

Dr. Imbriale is a Fellow of the IEEE and has an extensive list of publications.

Eric Gama *is a member of the engineering staff in the Communications Ground System Section at the Jet Propulsion Laboratory (JPL) in Pasadena California. A graduate of the California State University Los Angeles School of Engineering and Technology, he has a Bachelor of Science degree in Mechanical Engineering. Starting in 1998 at JPL as an academic part time (APT) employee, he has worked on the research and development of gossamer structures as a way of reducing launch payload and volume, for use on space deployable, reflect-array antennas. Since beginning his full-time status at JPL, he has been part of the Antenna Mechanical and Structural Engineering Group responsible for the mechanical design and maintenance of the large aperture antennas of NASA's Deep Space Network (DSN).*